ACS Catalysis

Letter

pubs.acs.org/acscatalysis

Zeolite Structural Confinement Effects Enhance One-Pot Catalytic Conversion of Ethanol to Butadiene

Weili Dai,[†] Shanshan Zhang,[†] Zhiyang Yu,[§] Tingting Yan,[†] Guangjun Wu,[†] Naijia Guan,[†,‡] and Landong Li*[,†,‡]

[†]School of Materials Science and Engineering and National Institute for Advanced Materials, Nankai University, Tianjin 300071, China

[‡]Key Laboratory of Advanced Energy Materials Chemistry of Ministry of Education, Collaborative Innovation Center of Chemical Science and Engineering, Nankai University, Tianjin 300071, China

[§]School of Materials Science and Engineering, Xiamen University of Technology, Xiamen 361024, China

S *Supporting Information*

ABSTRACT: The one-pot conversion of ethanol to butadiene is a promising route for butadiene production; however, simultaneous attainment of high butadiene productivity and high butadiene selectivity is challenging. Here, zeolite-confined bicomponent Zn−Y clusters were constructed and applied as robust catalysts for ethanol-to-butadiene conversion with a state-of-the-art butadiene productivity of 2.33 $g_{BD}/g_{cat}/h$ and butadiene selectivity of ∼63%. Structural confinement effects are responsible for the enhanced butadiene production efficiency via a multiple-step cascade reaction.

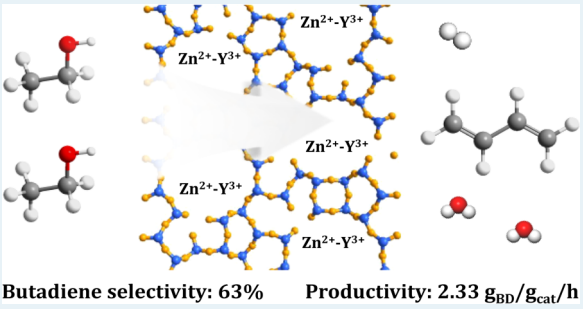

KEYWORDS: *ethanol-to-butadiene, zeolite, confinement effects, catalysis, cascade reaction*

1,3-Butadiene is an important industrial chemical used as a monomer in the production of synthetic rubber. Currently, the global production of butadiene amounts to more than 10 million tons per year, and most of the butadiene is produced via the extractive distillation of C4 fractions from naphtha steam-cracking processes.[1] To expand the source of butadiene production and improve its excessive dependence on steam cracking, alternative routes for butadiene production, e.g. from dehydrogenation of *n*-butane or butenes and from ethanol conversion, have been explored. The one-pot conversion of ethanol to butadiene was developed by Sergei Lebedev,[2] commercialized in Russia in the 1920s, and unfortunately abandoned after 1960s because of economic considerations. With the recent increase in ethanol production, especially the rapid development of bioethanol, the Lebedev process is becoming a competitive route for butadiene production[3] and therefore attracts renewed research interests.[4−7]

The mechanism and reaction network of ethanol-to-butadiene conversion have been extensively investigated in the past decades. Through sufficient debates, several key reaction steps are now generally accepted (Scheme 1),[8] including (i) the dehydrogenation of ethanol to acetaldehyde, (ii) the aldol condensation of acetaldehyde to acetaldol, (iii) the dehydration of acetaldol to crotonaldehyde, (iv) the Meerwein−Ponndorf−Verley reduction of crotonaldehyde to crotyl alcohol, and (v) the dehydration of crotyl alcohol to butadiene. Obviously, this is a very complicated reaction process and catalysts with multiple functionalities are required.

Scheme 1. Reaction Network of Ethanol-to-Butadiene Conversion

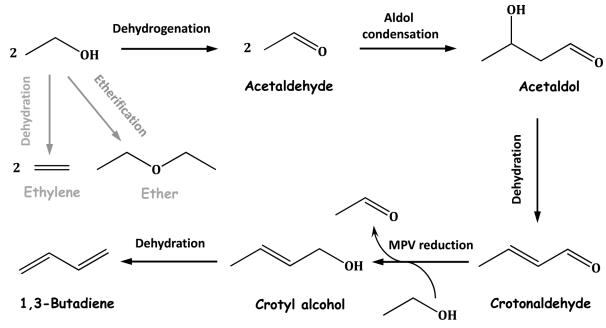

The key to the success of ethanol-to-butadiene process is the simultaneous attainment of a high butadiene productivity for practical operation and a high butadiene selectivity to avoid the expensive and time-consuming purification steps, which remains very challenging.

In the present study, we introduce the confinement effects to ethanol-to-butadiene catalysts by using zeolite as a catalyst support, and we demonstrate that such a simple strategy can significantly enhance the butadiene production efficiency to a

Received: February 9, 2017
Revised: April 21, 2017
Published: April 24, 2017

DOI: 10.1021/acscatal.7b00433
ACS Catal. 2017, 7, 3703−3706

Table 1. Ethanol Conversion to Butadiene over Confined Catalysts

				product selectivity (mol %)[a]				
catalyst	T (K)	conversion (%)	productivity ($g_{BD}/g_{cat}/h$)[a]	C_2H_4	$C_2H_5OC_2H_5$	CH_3CHO	crotonaldehyde	C_4H_6
5%Zn/beta	623	81	0.21	14	4	33	5	33
5%Cu/beta	623	93	0.01	44	8	44	1	1
5%Y/beta	623	93	0.03	95	0	0	0	5
5%Ce/beta	623	78	0.09	78	8	0	0	14
5%Cu-5%Y/beta	623	50	0.07	0	25	0	0	19
5%Cu-5%Ce/beta	623	80	0.20	10	0	38	12	33
5%Zn-5%Ce/beta	623	87	0.46	10	0	8	2	66
5%Zn-5%Y/beta	623	89	0.50	8	2	4	1	69
2%Zn-8%Y/beta	623	92	0.53	9	3	1	1	74
2%Zn-8%Y/beta[b]	623	100	0.12	17	0	0	0	75
2%Zn-8%Y/beta[b]	603	90	0.11	12	0	0	0	81
2%Zn-8%Y/beta[c]	623	47	1.46	7	5	6	4	67
2%Zn-8%Y/beta[c]	673	82	2.33	12	2	7	3	63

[a]WHSV = 1.3/h unless specifically stated; data recorded at reaction for 1 h. [b]WHSV = 0.3/h. [c]WHSV= 7.9/h.

new level. The concept of confined catalysis might also be applicable to a wide range of multiple-step cascade reactions for industrial chemical production.

The zeolite-confined catalyst systems were constructed via a postsynthesis route on the basis of our previous work.[9] Briefly, zeolite H-beta was fully dealuminated and then mixed with an approximate amount of decomposable metal precursors (usually nitrates). Upon calcination, the metal precursors decomposed and reacted with the silanols created from dealumination. In such a way, metal functional sites could be introduced into zeolite cages, locating at former Al positions of parent zeolite, to build confined catalytic reactors, as supported by ^{29}Si MAS NMR spectra (Figure S1) and DRIFT spectra (Figure S2) The ethanol conversion over various confined monocomponent zeolite catalysts was first studied in a fixed-bed reactor, and the results are shown in Supplementary Figure S3. Transition-metal components Cu, Zn, and Ag appear to be active for ethanol dehydrogenation to acetaldehyde; however, the Ag catalyst suffers from severe activity loss with the progress of reaction. Rare-earth metal components Y, La, Ce, Pr, and Nd seem to be active for acetaldehyde conversion because a significant amount of butadiene could be detected in the product while no acetaldehyde was detected. This is verified by the experimental results from acetaldehyde condensation over representative rare-earth metal catalysts (Figure S4). We then come to the idea of combining the ethanol dehydrogenation component with acetaldehyde condensation component for the one-step ethanol conversion to butadiene. As expected, bicomponent zeolite catalysts exhibited greatly enhanced efficiency in ethanol-to-butadiene conversion (Table 1). For 5%Zn-5%Y/beta, a high butadiene productivity of 0.50 $g_{BD}/g_{cat}/h$ with a butadiene selectivity of 69% could be achieved. Optimizing the catalyst composition (Figure S5) and reaction conditions (Figure S7) could further increase the butadiene production efficiency to a great extent. Typically, a stable high butadiene selectivity of ~81% (12% ethylene and 7% propylene as byproduct) with butadiene productivity of 0.11$g_{BD}/g_{cat}/h$ can be achieved at WHSV of 0.3/h and temperature of 603 K over bicomponent 2%Zn-8%Y/beta. Alternatively, a state-of-the-art butadiene productivity of 2.33 $g_{BD}/g_{cat}/h$ with a high butadiene selectivity of ~63% (see Table S1 and Figure S8 for direct comparison with literature results) can be achieved at WHSV of 7.9/h and temperature of 673 K over the same catalyst. Moreover, the bicomponent 2%Zn-8%Y/beta can be fully regenerated via a simple calcination process (Figure S9), demonstrating its potential for industrial ethanol-to-butadiene conversion in a circulating fluidized bed reactor.

For reference, 5%Zn-5%Y/SiO_2 and 5%Zn-5%Y/MCM-41 were prepared and investigated for ethanol-to-butadiene conversion. The structures of supported bicomponent catalysts are confirmed by XRD analysis (Figure S10). The absence of diffraction patterns corresponding to ZnO or Y_2O_3 indicates the good dispersion of Zn and Y species even at high loading employed. The pore sizes of 5%Zn-5%Y/SiO_2, 5%Zn-5%Y/MCM-41, and 5%Zn-5%Y/beta are determined to be 24, 2.8, and 0.8 nm, respectively (Figure S11). That is, the functional sites Zn−Y are confined in micropores (beta: 0.8 nm), mesopores (MCM-41:2.8 nm), and macropores (SiO_2: 24 nm) of silica support, respectively. All silica-supported bicomponent Zn−Y catalysts are active for the ethanol-to-butadiene conversion; however, their catalytic performance differs a lot (Figure 1). The highest initial butadiene productivity of 0.52 $g_{BD}/g_{cat}/h$ is achieved on 5%Zn-5%Y/beta, followed by the 0.15 $g_{BD}/g_{cat}/h$ on 5%Zn-5%Y/MCM-41, and then 0.10 $g_{BD}/g_{cat}/h$ on 5%Zn-5%Y/SiO_2 under identical reaction conditions. Because ethanol-to-butadiene is a multiple-step reaction and a specific functional site is required for an individual step (Scheme 1), an effective transfer of the intermediate product from one site to the next is a key issue for the high productivity of butadiene. This is guaranteed by the formation of Zn−Y-containing clusters confined in zeolite channels (vide infra). With the close contact between different functional sites, the intermediate product acetaldehyde has a higher chance to react with each other to produce acetaldol rather than escape as unwanted byproduct. Meanwhile, the byproduct acetaldehyde may bear diffusion resistance within zeolite channels, which further improve the aldol condensation of acetaldehyde. Undoubtedly, ordered and limited space is expected to provide a better confinement effect, and in this context, three-dimensional zeolite cages should be the ideal choice. In the reaction of ethanol-to-butadiene, the selectivity to acetaldehyde can be used as an indicator of confinement effect: higher acetaldehyde selectivity means weaker confinement effect and, accordingly, lower butadiene productivity.

For a better understanding of the support structural confinement effects in bicomponent catalysts, high-resolution XPS and TEM analysis was performed. The binding energy values of 1023.9 and 1047.0 eV, corresponding to Zn $2p_{3/2}$ and

DOI: 10.1021/acscatal.7b00433
ACS Catal. 2017, 7, 3703−3706

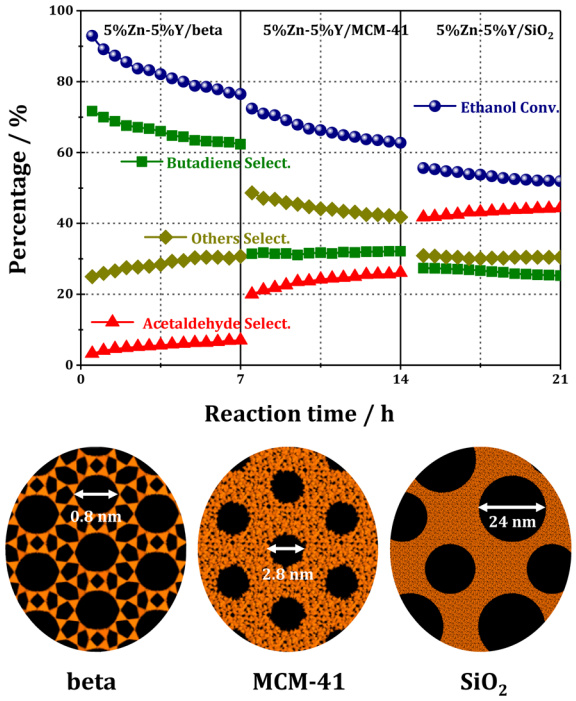

Figure 1. Ethanol-to-butadiene conversion catalyzed by 5%Zn-5%Y/SiO_2 and 5%Zn-5%Y/MCM-41 and 5%Zn-5%Y/beta, with the schematic diagrams of support confinement effects. Reaction conditions: 0.3 g catalyst, WHSV = 1.3/h, T = 623 K.

$2p_{1/2}$, respectively, are observed for monocomponent Zn/beta. These values are significantly higher than reference bulk ZnO (1022.1 and 1045.2 eV, Figure S12), which is due to the formation of the Si−O−Zn bond (Si−O− as electron-withdrawing ligand). For bicomponent Zn−Y on silica support, similar binding energy values at 1023.2 and 1046.4 eV are observed (Figure 2, left chart). The shift toward lower values

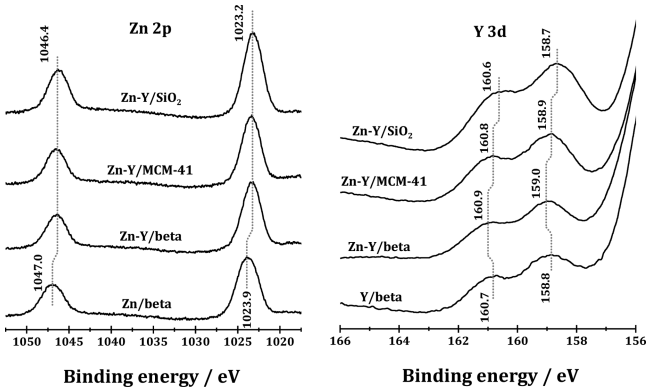

Figure 2. High-resolution Zn 2p and Y 3d XPS of selected samples.

compared to bicomponent Zn/beta should be due to the electron transfer from Y to Zn and/or the reduced Si−O−Zn bond by the presence of Y. In the Y 3d XPS (Figure 2, right chart), binding energy values of 158.8 and 160.7 eV corresponding to Y $3d_{5/2}$ and $3d_{3/2}$, respectively, are observed for monocomponent Y/beta, which are distinctly higher than bulk Y_2O_3 (156.7 and 158.6 eV, Figure S12), which is due to the formation of the Si−O−Y bond. In contrast, binding energy values of 159.0 and 160.9 eV corresponding to Y $3d_{5/2}$ and $3d_{3/2}$, respectively, are observed for bicomponent Zn−Y/beta. The shift toward higher values compared to monocomponent Y/beta is originated from the balance between the electron transfer from Y to Zn and the reduced Si−O−Y bond by the presence of Zn. Obviously, the electron transfer from Y to Zn plays the leading role in the process, which also indicates the strong interaction between Zn and Y in bicomponent Zn−Y/beta catalyst. For bicomponent Zn−Y/MCM-41 and Zn−Y/SiO_2, the Y 3d binding energy shift toward lower values compared to Zn−Y/beta, but still distinctly higher than bulk Y_2O_3. This should be explained from the weaker interaction between Zn and Y in Zn−Y/MCM-41 and Zn−Y/SiO_2 as compared to Zn−Y/beta, as well as the formation of Si−O−Y bonds in all bicomponent Zn−Y on silica supports. In a whole, XPS results reveal the interaction between Zn and Y species in bicomponent Zn−Y catalysts and a stronger interaction between Zn and Y is observed in Zn−Y/beta with stronger structural confinement effects.

The catalytically active Zn−Y species on different silica supports was investigated by means of electron microscopy. Bright-field HRTEM image of 5%Zn-5%Y/beta shows clear lattice fringes of zeolite support but no evidence of Zn−Y species on the support (Figure S13). Figure 3a shows the

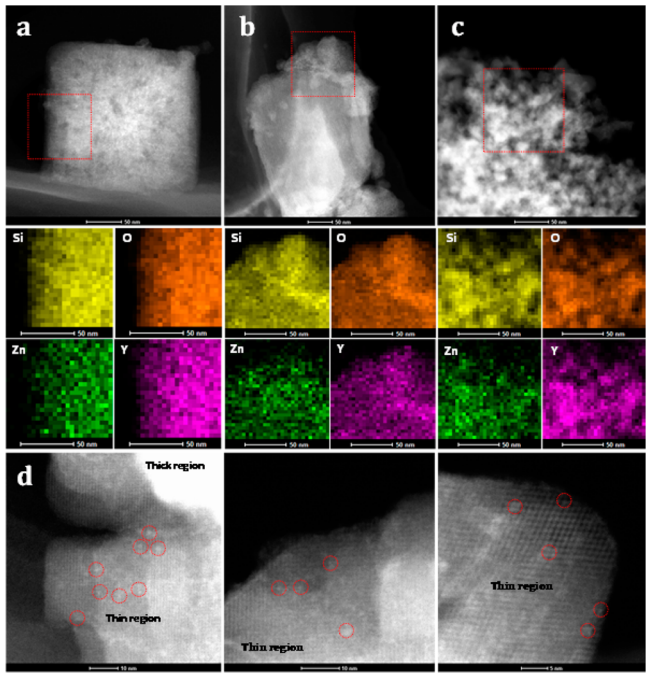

Figure 3. HAADF-STEM images with corresponding element mapping of 5%Zn-5%Y/beta (a), 5%Zn-5%Y/MCM-41 (b), and 5% Zn-5%Y/SiO_2 (c); representative high-resolution HAADF-STEM images of 5%Zn-5%Y/beta sample (d).

representative STEM image of 5%Zn-5%Y/beta acquired in the high-angle-dark-field (HAADF) detection mode. The corresponding element mapping results confirm the homogeneous distribution of Zn and Y species as well as their close contact. In contrast, although the homogeneous distribution of Zn or Y species is achieved for 5%Zn-5%Y/MCM-41 and 5%Zn-5%Y/SiO_2 with metal loading below monolayer coverage,[10] the enrichment in Zn or Y in specific regions can be observed (Figure 3b,c), which would unavoidably lead to low catalytic efficiency in multiple-step reactions. In the high-resolution HAADF-STEM images of 5%Zn-5%Y/beta (Figure 3d), bright

DOI: 10.1021/acscatal.7b00433
ACS Catal. 2017, 7, 3703−3706

flecks with diameters of ~0.5−2 nm are observed to distribute on zeolite support (highlighted by red circles in the thin region), indicating the formation of clusters. Unfortunately, Zn and Y atoms cannot be solved by HAADF imaging; however, energy dispersive spectroscopy analysis does reveal the presence of both Zn and Y in a single cluster (Figure S16). The diameter of Zn−Y cluster is consistent with the cage of beta zeolite (although larger nanoparticles might also exist), and it can be stated that Zn−Y clusters are formed owing to zeolite structural confinement effects. Such Zn−Y clusters exhibit attracting activity in the one-pot conversion of ethanol to butadiene (Figure 1, Table 1, and Table S1).

In summary, bicomponent Zn−Y clusters were constructed by using zeolite beta with structural confinement effect as a catalyst support. Bicomponent Zn−Y clusters confined in zeolite cages exhibited a state-of-the-art butadiene productivity of 2.33 $g_{BD}/g_{cat}/h$ with a high butadiene selectivity of ~63% in the one-pot ethanol-to-butadiene conversion, which can meet industrialization production requirements of butadiene. Structural confinement effects should be developed as a general strategy to enhance the catalytic efficiency for chemical production via multiple-step reactions.

■ ASSOCIATED CONTENT

Supporting Information

The Supporting Information is available free of charge on the ACS Publications website at DOI: 10.1021/acscatal.7b00433.

Additional catalyst preparation, characterization, and reaction data are provided (PDF)

■ AUTHOR INFORMATION

Corresponding Author

*E-mail for L.D.L.: lild@nankai.edu.cn.

ORCID

Weili Dai: 0000-0001-5752-0662

Landong Li: 0000-0003-0998-4061

Notes

The authors declare no competing financial interest.

■ ACKNOWLEDGMENTS

This work was supported by the National Natural Science Foundation of China (21573113, 21421001) and Municipal Natural Science Foundation of Tianjin (16JCQNJC04900, 13RCGFGX01124).

■ REFERENCES

(1) White, W. C. *Chem.-Biol. Interact.* **2007**, *166*, 10−14.

(2) (a) Lebedev, S. V. British Patent 331402, 1929. (b) Lebedev, S. V. British Patent 331482, 1930.

(3) (a) Patel, A. D.; Meesters, K.; den Uil, H.; de Jong, E.; Blok, K.; Patel, M. K. *Energy Environ. Sci.* **2012**, *5*, 8430−8444. (b) Angelici, C.; Weckhuysen, B. M.; Bruijnincx, P. C. A. *ChemSusChem* **2013**, *6*, 1595−1614. (c) Makshina, E. V.; Dusselier, M.; Janssens, W.; Degreve, J.; Jacobs, P. A.; Sels, B. F. *Chem. Soc. Rev.* **2014**, *43*, 7917−7953.

(4) (a) Ohnishi, R.; Akimoto, T.; Tanabe, K. *J. Chem. Soc., Chem. Commun.* **1985**, 1613−1614. (b) Makshina, E. V.; Janssens, W.; Sels, B. F.; Jacobs, P. A. *Catal. Today* **2012**, *198*, 338−344. (c) Angelici, C.; Velthoen, M. E. Z.; Weckhuysen, B. M.; Bruijnincx, P. C. A. *ChemSusChem* **2014**, *7*, 2505−2515. (d) Lewandowski, M.; Babu, G. S.; Vezzoli, M.; Jones, M. D.; Owen, R. E.; Mattia, D.; Plucinski, P.; Mikolajska, E.; Ochenduszko, A.; Apperley, D. C. *Catal. Commun.* **2014**, *49*, 25−28. (e) Larina, O. V.; Kyriienko, P. I.; Soloviev, S. O. *Catal. Lett.* **2015**, *145*, 1162−1168. (f) Janssens, W.; Makshina, E. V.; Vanelderen, P.; De Clippel, F.; Houthoofd, K.; Kerkhofs, S.; Martens, J. A.; Jacobs, P. A.; Sels, B. F. *ChemSusChem* **2015**, *8*, 994−1008. (g) Shylesh, S.; Gokhale, A. A.; Scown, C. D.; Kim, D.; Ho, C. R.; Bell, A. T. *ChemSusChem* **2016**, *9*, 1462−1472. (h) Chung, S.-H.; Angelici, C.; Hinterding, S. O.M.; Weingarth, M.; Baldus, M.; Houben, K.; Weckhuysen, B. M.; Bruijnincx, P. C.A. *ACS Catal.* **2016**, *6*, 4034−4045.

(5) (a) Jones, M. D.; Keir, C. G.; Iulio, C. D.; Robertson, R. A. M.; Williams, C. V.; Apperley, D. C. *Catal. Sci. Technol.* **2011**, *1*, 267−272. (b) Sushkevich, V. L.; Ivanova, I. I.; Ordomsky, V. V.; Taarning, E. *ChemSusChem* **2014**, *7*, 2527−2536. (c) De Baerdemaeker, T.; Feyen, M.; Müller, U.; Yilmaz, B.; Xiao, F.-S.; Zhang, W.; Yokoi, T.; Bao, X. H.; Gies, D. E.; De Vos, D. E. *ACS Catal.* **2015**, *5*, 3393−3397. (d) Baylon, R. A. L.; Sun, J.; Wang, Y. *Catal. Today* **2016**, *259*, 446−452.

(6) (a) Sushkevich, V. L.; Ivanova, I. I.; Taarning, E. *Green Chem.* **2015**, *17*, 2552−2559. (b) Sushkevich, V. L.; Palagin, D.; Ivanova, I. I. *ACS Catal.* **2015**, *5*, 4833−4836. (c) Sushkevich, V. L.; Ivanova, I. I. *ChemSusChem* **2016**, *9*, 2216−2225. (d) Klein, A.; Keisers, K.; Palkovits, R. *Appl. Catal., A* **2016**, *514*, 192−202. (e) Kyriienko, P. I.; Larina, O. V.; Soloviev, S. O.; Orlyk, S. M.; Dzwigaj, S. *Catal. Commun.* **2016**, *77*, 123−126.

(7) (a) Sekiguchi, Y.; Akiyama, S.; Urakawa, W.; Koyama, T.; Miyaji, A.; Motokura, K.; Baba, T. *Catal. Commun.* **2015**, *68*, 20−24. (b) Hayashi, Y.; Akiyama, S.; Miyaji, A.; Sekiguchi, Y.; Sakamoto, Y.; Shiga, A.; Koyama, T.; Motokura, K.; Baba, T. *Phys. Chem. Chem. Phys.* **2016**, *18*, 25191−25209.

(8) (a) Jones, H. E.; Stahly, E. E.; Corson, B. B. *J. Am. Chem. Soc.* **1949**, *71*, 1822−1828. (b) Kvisle, S.; Aguero, A.; Sneeden, R. P. A. *Appl. Catal.* **1988**, *43*, 117−131. (c) Chieregato, A.; Ochoa, J. V.; Bandinelli, C.; Fornasari, G.; Cavani, F.; Mella, M. *ChemSusChem* **2015**, *8*, 377−388. (d) Angelici, C.; Meirer, F.; van der Eerden, A. M. J.; Schaink, H. L.; Goryachev, A.; Hofmann, J. P.; Hensen, E. J. M.; Weckhuysen, B. M.; Bruijnincx, P. C. A. *ACS Catal.* **2015**, *5*, 6005−6015.

(9) (a) Tang, B.; Dai, W.; Sun, X.; Guan, N.; Li, L.; Hunger, M. *Green Chem.* **2014**, *16*, 2281−2291. (b) Tang, B.; Dai, W.; Wu, G.; Guan, N.; Li, L.; Hunger, M. *ACS Catal.* **2014**, *4*, 2801−2810. (c) Tang, B.; Dai, W.; Sun, X.; Wu, G.; Guan, N.; Hunger, M.; Li, L. *Green Chem.* **2015**, *17*, 1744−1755. (d) Dai, W.; Wang, C.; Tang, B.; Wu, G.; Guan, N.; Xie, Z.; Hunger, M.; Li, L. *ACS Catal.* **2016**, *6*, 2955−2964.

(10) (a) Wachs, I. E. *Catal. Today* **2005**, *100*, 79−94. (b) Wachs, I. E.; Keturakis, C. J. In: Monolayer Systems. *Comprehensive Inorganic Chemistry II*; Reedijk, J., Poeppelmeier, K., Eds.; Elsevier: Amsterdam, 2013; Vol. 7; pp 131−151.

DOI: 10.1021/acscatal.7b00433
ACS Catal. 2017, 7, 3703−3706